

CHRNA5 D398N mutation in addiction: Pathogenic insights and therapeutic discovery

Mohd Imran^{1,2}, Maria Kafayat³, Muhammad Umer Khan³, Lina Eltaib⁴, Saooda Ibrahim^{5,6}, Abdullah R. Alzahrani⁷, Howayada Mahany Mostafa⁸ and Imran Waheed^{9*}

¹Center for Health Research, Northern Border University, Arar 73213, Saudi Arabia.

²Department of Pharmaceutical Chemistry, College of Pharmacy, Northern Border University, Rafha 91911, Saudi Arabia.

³Institute of Molecular Biology and Biotechnology, The University of Lahore, Lahore, Pakistan

⁴Department of Pharmaceutics, College of Pharmacy, Northern Border University, Rafha, Saudi Arabia

⁵Institute of Molecular Biology and Biotechnology, The University of Lahore, Lahore, Pakistan

⁶Centre for Applied Molecular Biology, University of the Punjab, Lahore, Pakistan

⁷Department of Pharmacology and Toxicology, Faculty of Medicine, Umm Al-Qura University, Al-Abidiyah, Makkah, Saudi Arabia

⁸Department of Chemistry, College of Science, Northern Border University, Arar, Saudi Arabia

⁹Akhtar Saeed College of Pharmacy, Canal Campus, Lahore, Pakistan

Abstract: Background: Drug addiction is a significant public health issue, with genetic components playing a role in predisposing a person to susceptibility. **Objective:** the current study planned to investigate the pathogenic potential of the CHRNA5 D398N (rs16969968) mutation and computationally identify structurally optimized aripiprazole analogs capable of selectively binding the mutant protein. **Methods:** PolyPhen-2 and AlphaMissense were used to assess the pathogenic impact of the D398N (rs16969968) mutation in CHRNA5. SwissSimilarity was employed to identify aripiprazole-like structural analogs for therapeutic screening. The chemical structures of selected analogs were drawn and optimized using ChemDraw. SwissADME was used to evaluate pharmacokinetic properties, including drug-likeness and absorption parameters. Molecular docking was performed to estimate the binding affinity of candidate ligands toward the mutant CHRNA5 protein, while Density Functional Theory (DFT) analysis was conducted to determine their electronic, reactive, and electrostatic properties for final lead selection. **Results:** Functional prediction tools, including PolyPhen-2 and Alpha Missense, predict the mutation to be pathogenic with high scores predicting deleterious effects. Structural modeling with AlphaFold showed conformational changes in the mutant CHRNA5 protein, especially at the active site, validated with structural alignment. For therapeutic potential, 20 structurally similar aripiprazole ligands were identified through Swiss Similarity. Molecular docking indicated ligand 12 and ligand 4 had the highest binding affinity for mutant protein (−3.034 and −2.774 kcal/mol, respectively). PyMOL visualization indicated ligand-receptor interactions. ADMET analysis predicted good pharmacokinetics: Ligand 12 indicated high gastrointestinal absorption and CYP non-inhibition, while ligand 4 was a non-P-gp substrate with good solubility. DFT analysis indicated ligand 4 was the most polar, while ligand 12 was the most chemically reactive. **Conclusion:** These findings imply the D398N mutation predisposes to addiction susceptibility and that ligand 12 holds promise as a therapeutic target due to its high binding affinity and good pharmacological profiles.

Keywords: Addiction; CHRNA5; DFT; Drug Abuse; Molecular Docking; Mutation

Submitted on 29-01-2025 – Revised on 12-05-2025 – Accepted on 27-06-2025

INTRODUCTION

In the intricate world of forensic science, researchers strive to unravel the complexities of drug abuse, focusing on the molecular and genetic frameworks underpinning addiction. Among the various genetic contributors, the CHRNA5 gene, encoding the $\alpha 5$ subunit of nicotinic acetylcholine receptors (nAChRs), has garnered significant attention due to its modulatory role in receptor functionality and neurobehavioral outcomes related to addiction (Yang *et al.*, 2023). These receptors function as cationic ligand-gated ion channels, forming homo- or hetero-pentameric structures through different combinations of subunits. The CHRNA5-A3-B4 gene cluster, located on chromosome 15q25, encodes the $\alpha 5$, $\alpha 3$ and $\beta 4$ subunits. Variations in

these subunits influence the functional properties of nAChRs, impacting receptor composition, neurotransmission and behavioural outcomes (Chaity and Apu, 2022; Chaity *et al.*, 2021; Icick *et al.*, 2020). The mammalian nervous system has six α ($\alpha 2$ - $\alpha 7$) and three β ($\beta 2$ - $\beta 4$) nAChRs subunits. Acetylcholine binding in α subunits, but not in β subunits, requires conserved cysteines, such as residues 192-193 of the muscle $\alpha 1$ subunit. Research indicates that the $\alpha 3$ subunit mostly interacts with $\beta 4$ to form receptors like $\alpha 3\beta 4$, which are expressed in areas of the brain like the medial habenula and the interpeduncular nucleus (IPN). These receptors are essential for cholinergic modulation. Although the $\alpha 5$ subunit is called an "accessory subunit," it neither alone nor in conjunction with another subunit produces functional receptors. Instead, it modifies the receptor's functional

*Corresponding author: e-mail: imranwaheed81@hotmail.com

properties. Its presence in receptors like $\alpha 4\beta 2$ or $\alpha 3\beta 4$ alters ion channel activity and ligand binding, which significantly affects the functionality of nAChR (Icick *et al.*, 2020).

Importantly, a functional single nucleotide polymorphism (SNP) in CHRNA5, rs16969968, results in a D398N substitution, which has been linked in numerous studies to heavy nicotine consumption, nicotine dependence and an increased risk of lung cancer (Scholze and Huck, 2020). Remarkably, it also has a protective function against cocaine dependence, possibly because of its ability to regulate receptor activation (Aroche *et al.*, 2020). Long-term smoking causes nicotine dependency, a complex behavioural condition characterised by tolerance, cravings, withdrawal symptoms and an inability to control smoking despite negative effects. The effects of nicotine are produced via binding to nAChRs, which are mostly located in the central parts of the brain. Interestingly, nicotine's rewarding and addiction-related effects rely on the $\alpha 4$ subunit and the $\alpha 4\beta 2$ subtype of nAChRs has a high affinity for nicotine (Muderrisoglu *et al.*, 2022; Sansone *et al.*, 2023). In addition to increasing nicotine use and dependency, alterations in the CHRNA5-A3-B4 cluster can significantly impact gene expression and receptor function (Chaity and Apu, 2022; Chaity *et al.*, 2021; Schlaepfer *et al.*, 2008). Research on CHRNA5 has primarily examined nicotine addiction, with mixed results regarding its role in alcohol addiction (Brynildsen and Blendy, 2021). In a recent study among Bengali male smokers, it was determined that the rs16969968 allele of the CHRNA5 gene is implicated in heightened risk for nicotine dependence. Smokers with the AA genotype of the SNP had greater chances of developing dependence, measured using both FTND and CDS-12 scores. Even though the correlations were not extremely strong statistically, the results point toward a probable implication of rs16969968 in modulating nicotine addiction in this group (Chaity and Apu, 2022).

Some research suggests that CHRNA5 polymorphisms may reduce alcohol-related symptoms, but other studies find no significant associations, highlighting the complexity of genetic factors influencing substance addiction disorders (Brynildsen and Blendy, 2021). Despite extensive studies on CHRNA5 in nicotine addiction, its broader implications in general drug abuse remain unclear. Moreover, limited research has focused on its molecular interactions or its association with addiction in specific population. This creates a critical research gap in understanding the gene's comprehensive role in addiction biology. The purpose of this study is to investigate whether drug addiction behaviors and specific mutations in CHRNA5, namely the D398N variant (rs16969968), are associated with drug addiction behavior in a target population. We will examine genetic profiles and evaluate molecular interactions to see whether CHRNA5 variants are more prevalent in people who have a propensity for

drug use. This study intends to find genetic markers that contribute to this population's susceptibility to addiction to better understand the molecular mechanisms behind addiction. The findings are meant to guide the development of targeted therapeutic interventions, tailored treatment programs and effective public health measures to address addiction in the region.

MATERIALS AND METHODS

Data collection

This study aimed to examine how CHRNA5 mutations affect the likelihood of developing a drug addiction using genetic analysis and computational techniques. PubChem, NCBI, Google Scholar, PubMed, Springer, MDPI, Wiley Online Library, Taylor & Francis and Scopus were among the many sites that were used to collect the data. We used keywords such as "missense," "CHRNA5," "drug abuse," "addiction," and "docking" to identify relevant genes and significant hotspot changes. A variety of *in silico* techniques were used in the analysis to investigate the connection between genetic changes in CHRNA5 and their possible involvement in addiction. The study was noteworthy for highlighting hotspot alterations, such as the D398N variation (rs16969968), which may be important in the setting of drug addiction.

In-Silico functional and structural analysis of mutation

In silico analysis was performed using a range of bioinformatics tools and databases. Functional Predictions were made using SIFT (<https://sift.bii.a-star.edu.sg/>) and PolyPhen-2 (<https://genetics.bwh.harvard.edu/pph2/>) to predict the effects of amino acid substitutions on protein function (Sim *et al.*, 2012; Flanagan *et al.*, 2010; Shan *et al.*, 2024). For Structural Analysis, the protein structure was retrieved from UniProt, the Universal Protein Knowledgebase, with the ID 'P30532 · ACHA5_HUMAN' (<https://www.uniprot.org/>). CHRNA5 is composed of 468 amino acids.

Docking analysis

To prepare the protein for further analysis, all chains, except for chain A, were removed using BIOVIA Discovery Studio Visualizer v21.1.0.20298 (Milne, 2010; Systèmes, 2021). The protein structure was processed using Schrödinger's 2020-3 suite, specifically through the Protein Preparation Wizard in Maestro Wizard (version 21.3). A mutation at position 398 of the protein was introduced (D398N), using Schrödinger's 2020-3 suite (Maestro Wizard version 21.3) (Maestro, 2020). The docking sites were determined using the Schrödinger's SiteMap module. To determine the binding cavity of the target protein for docking, the "Receptor grid Generation" panel of Maestro 12.5 was utilized. The compounds were then docked into the grid structure generated, which is indicative of the binding cavity of the protein. The reference drug, aripiprazole, was selected because it is used clinically in rehabilitation centers and drug addiction treatment settings for substance use disorders (Moran L *et*

al., 2017). It provides a model to screen for structurally analogous ligands that have the potential to bind to the mutated CHRNA5 protein and provide therapeutic promise for drug addiction. For the retrieval and preparation of ligands, reference compound data was made using Zinc database on Swiss Similarity for identifying structurally similar compounds. The 2D and 3D structures of selected ligands were sourced from PubChem, created using ChemDraw (Version 21.0) and visualized using Discovery Studio Visualizer (v21.1.0.20298) (Milne, 2010; Systèmes, 2021). Ligands were prepared with the LigPrep program in Maestro 12.5, using the OPLS3e force field at pH 7.0 ± 2 . Epik was employed to create potential protonation and tautomeric states. Stereoisomer generation was turned on, maintaining defined chiral centers with variation allowed at others, generating up to 10 stereoisomers per compound (Uniyal and Mahapatra, 2022). All compounds were docked into the binding cavity by employing Maestro 12.5. A grid file was imported and the pre-prepared compounds were loaded into the ligand docking panel. Docking was conducted employing flexible docking with XP (Extra Precision) mode, along with XP descriptor instructions for enhanced accuracy. Other settings included calculation of per-residue binding scores at a 12.0 Å radius and RMSD for geometries of input compounds. Following dock analysis, docked structures were merged and stored in PDB format and docking scores were extracted and stored in CSV file format to be analyzed. The PyMOL (Version 2.4.0.) used for complex visualization (Maestro, 2020).

Evaluation of drug profile through ADME and toxicity analyses

The ADMET analysis in terms of absorption, distribution, metabolism, excretion and toxicity was performed using SwissADME server (SwissADME), which assesses compounds based on pharmacokinetic behavior and drug-likeness. The compounds' drug-likeness was evaluated using Lipinski's Rule of Five (RO5), along with other filters such as Ghose, Veber, Egan and Muegge rules. After entering the SMILES string for the compound, ADME analysis was carried out (Islam *et al.*, 2024; Rauf *et al.*, 2025).

Density functional theory (DFT) studies

DFT computations were performed using the Gaussian 06 package, with the RB3LYP function and the SVP basis set. This approach was chosen because of its stable trade-off between computational expense and accuracy for describing the electronic structures of bioactive compounds. DFT was used to predict the reactivity, stability and electron distribution of the lead compound, which are critical in understanding its potential for interaction with target proteins at the molecular level. These computations assessed electronic structures, global/local reactivity descriptors, frontier molecular orbitals (HOMO and LUMO), molecular electrostatic potential (MEP) and optimal geometric parameters. Additionally, key molecular parameters were derived

based on Koopman's theorem to estimate the ionization potential and electron affinity of the compound. The results were analyzed using GaussView 6 (Silvarajoo *et al.*, 2020). The DFT calculations were slightly modified using the previously designated procedure (Bao F *et al.*, 2020). Utilizing the Gaussian 09 Revision D.01 with the default configuration, all calculations in the SVP basis set utilized the B3LYP function. Using this theory, the electronic structure of atoms and molecules can be effectively calculated. The present investigation will ascertain the optimized geometric parameters, molecular electrostatic potential (MEP), frontier molecular orbital (FMO) and global and local reactivity descriptors. The checks were examined utilizing Gauss View 5.0.8 software.

RESULTS

In Silico validation of sequence-based and structure-based analysis

According to the findings, the alpha5 subunit of the nicotinic acetylcholine receptor (CHRNA5) has the D398N mutation, which results in an amino acid change at position 398 from aspartic acid (D) to asparagine (N). The functional significance of this mutation was evaluated using predictive techniques. SIFT and PolyPhen-2 both determined that the mutation was benign; PolyPhen-2 reported a score of 0.0004 (Fig. S1). Nevertheless, with a score higher than 0.7, the AlphaMissense pathogenicity heatmap identified the mutation as harmful. To evaluate structural changes, the wild-type and mutated CHRNA5 protein structures were analyzed using AlphaFold, which provided high-accuracy predictions. Structural alignment conducted using the Basic Local Alignment Search Tool (BLAST) confirmed the accuracy of the wild-type sequence and the structural integrity of the predicted models. The analysis highlighted the presence of the D398N mutation in the mutated structure, marked as a distinct feature (Fig. 1; Fig. 2a, 2b).

In silico experimental validation of ADMET analysis

Absorption, Distribution, Metabolism, Excretion and Toxicity (ADMET) analysis was performed to evaluate the pharmacokinetic and toxicity profiles of ligands. Aripiprazole was chosen as the reference drug (Fig. S2) and 20 additional ligands were selected based on SwissADME scores exceeding 0.7. All ligands adhered to Lipinski's Rule of 5 (LPR, with molecular weights below 500 g/mol, fewer than 10 hydrogen bond acceptors (HBA) and fewer than 5 hydrogen bond donors (HBD). This is a sign of good drug-like potential in all the compounds. Ligands 6 and 13 exhibited poor solubility, with LogSw values of -6.62 and -6.75, respectively, whereas ligands 4 and 8 demonstrated relatively better solubility, with LogSw values of -3.31 and -3.84. Ligand 8, which displayed a favorable balance between solubility (-1.88 LogSw) and lipophilicity (Consensus Log P of 0.99), emerged as a promising candidate for further investigation. Analysis of lipophilicity revealed that ligands 6, 10 and 13 had

Consensus Log P values exceeding 2.5, indicating high lipophilicity and better membrane permeability. In contrast, ligands 2 and 4, with lower Consensus Log P values of 0.77 and -0.59, respectively, were predicted to have reduced permeability. Among the tested ligands, 16 were identified as substrates for P-glycoprotein (P-gp), including ligands 1, 2, 3, 5, 6, 7, 8, 10, 11, 12, 14, 16, 17, 18 and 19. Conversely, ligands 4, 9, 13, 15 and 20 were not substrates, suggesting better cellular retention and efficacy due to reduced P-gp-mediated efflux. Ligand mutations or structural changes affected important pharmacokinetic properties such as GI absorption, solubility and CYP interactions while still being Ro5 compliant. For example, ligands 2, 8 and 12 had good ADMET profiles, while ligand 4, although Ro5 compliant, had poor GI absorption, perhaps due to structural changes affecting membrane transport.

All ligands had no PAINS alerts, indicating no immediate concerns for assay interference. However, ligands 4 and 15 had one Brenk alert each, suggesting the presence of substructures potentially linked to toxicity. Inhibition of cytochrome P450 (CYP) enzymes was also evaluated, as these enzymes are key in drug metabolism. Ligands 1, 5, 8, 9, 10, 12, 13, 15, 17, 18 and 20 inhibited CYP2D6, posing risks of drug-drug interactions and metabolic complications. Furthermore, ligands 6, 7, 13, 15, 17 and 20 inhibited multiple CYP enzymes (CYP1A2, CYP2C19, CYP2C9, CYP2D6 and CYP3A4), indicating a higher potential for toxicity. In contrast, ligands 2, 3, 4, 8, 11, 14, 16 and 19 neither inhibited any CYP enzymes nor presented Brenk alerts, making them safer candidates with lower toxicity potential. In summary, ligands such as 2, 3, 8, 11, 14, 16 and 19, which showed no Brenk alerts and no CYP enzyme inhibition, had the lowest toxicity potential. Ligands 1, 5, 9, 10, 12 and 18 presented moderate toxicity risks due to CYP2D6 inhibition. Ligands 4, 6, 7, 13, 15, 17 and 20 exhibited higher toxicity potential due to multiple CYP enzyme inhibition and structural concerns. These findings underscore the importance of prioritizing ligands with favorable pharmacokinetic profiles and low toxicity for further development (Table 1).

Human intestinal absorption (HIA) analysis revealed that 19 ligands demonstrated high gastrointestinal absorption, which is critical for oral bioavailability. The "BOILED-Egg" plot predicted gastrointestinal absorption and blood-brain barrier (BBB) permeability. Compounds in the yellow region were predicted to cross the BBB, while those in the white region were identified as well-absorbed in the intestines (Fig. 3). To include practical drug-likeness aspects, predictions of solubility and bioavailability were examined for all ligands. Ligand 4 exhibited extremely high water solubility (log S: -0.78), which is indicative of its ease of formulation and absorption. It did, however, exhibit poor gastrointestinal (GI) absorption, which could restrict its oral bioavailability and necessitate formulation

adjustments. Contrarily, ligand 12 had good solubility (log S: -2.46) and high GI absorption, showing more potential for oral delivery and systemic availability. Both of the ligands were non-substrates of P-glycoprotein and non-permeable to the blood-brain barrier, which is a desirable feature in reducing off-target CNS effects. From these findings, ligand 12, especially, has a combination of favorable pharmacokinetic characteristics with high binding affinity, making it a candidate for further development.

In silico experimental validation of molecular docking

After the ADMET analysis, 20 top-performing compounds were selected as ligands and compared with the reference drug, aripiprazole. The SMILES notation for these ligands was generated using PubChem and visualized with ChemDraw and Discovery Studio. Structural visualization of both wild-type and mutated CHRNA5 proteins was performed using Discovery Studio to assess amino acid substitutions and their interactions within the protein. The identified ligands were subjected to docking with the mutated protein using Maestro software. Protein preparation involved optimization to remove water molecules, followed by grid generation around the active site predicted by the Site Finder tool at residue position 398 in the mutated CHRNA5 structure, defined by the x, y and z axes. Ligand preparation was also completed and the ligands, along with the reference drug, were docked with the mutated protein (Fig.S3). Redocking was performed to validate docking results and Root Mean Square Deviation (RMSD) values below 2 Å confirmed the reliability of the experiment. The dockiS1ng scores were analyzed to determine the ligands with the highest binding affinities. The reference drug achieved a docking score of -1.993, while several ligands demonstrated superior scores: ligand 12 scored -3.034, ligand 4 scored -2.774, ligand 2 scored -2.685, ligand 1 scored -2.450, ligand 15 scored -0.769, ligand 7 scored -2.198, ligand 20 scored -2.192, ligand 14 scored -2.129, ligand 9 scored -2.125 and ligand 8 scored -2.001 (Table 2). These ligands exhibited higher binding affinities with the mutated CHRNA5 protein structure compared to the reference drug, indicating strong interactions with key residues at the target site.

Molecular visualization of mutant and wild-type CHRNA5 structures with reference drug (Fig. 4) indicated differences in ligand binding and structural conformation. In the wild-type, aripiprazole formed stable contacts in an optimally defined binding pocket through hydrogen bonds, hydrophobic contacts and π - π stacking. The mutated structure, however, displayed varied positions of residues, forming different binding site geometries and interaction patterns. Aripiprazole was still docked but was altered by the mutation, changing the strength and character of the interactions, presumably to affect binding affinity and receptor function. As shown in Fig. 2, the D398N mutation of the CHRNA5 protein resides in a helical region, as

marked by the red dot in the mutant protein structure prediction (b). The site is likely to be in the transmembrane or ligand-binding region and the D398N mutation may alter the local structural environment critical for ligand interaction. In particular, the substitution of aspartic acid (negative charge residue) with asparagine (neutral polar residue) at position 398 may affect electrostatic interaction and hydrogen bonding with aripiprazole, modifying ligand binding affinity or orientation. To elucidate the molecular interactions, the fingerprint feature in Maestro was employed, mapping specific interactions between ligands and protein residues. The x-axis of the heat map represented amino acid residues (A376-A410), while the y-axis listed the ligands (0-20). Interaction strength was indicated by color intensity, with blue representing lower frequencies and red indicating higher frequencies. Ligands 12, 4, 2, 1 and 15 displayed distinct interaction profiles. Ligand 12 exhibited six total contacts, including five involving backbone atoms and six involving sidechain atoms, with five polar interactions, two charged interactions and two donor interactions, primarily engaging residues A400, A287, A329 and A300. Ligand 4 demonstrated five total contacts, including two backbone and five sidechain interactions, alongside four polar interactions, two charged interactions and two donor interactions, notably interacting with residues A300, A310, A327, A315 and A314. Ligand 2 showed six total contacts, including two backbone and six sidechain interactions, five polar interactions, three charged interactions and two donor interactions, engaging residues A401, A330, A289, A331 and A288. Ligand 1 displayed five total contacts, with four involving the backbone and five involving sidechain atoms, along with four polar interactions, two charged interactions and one donor interaction, involving residues A402, A290, A332, A291 and A287. Ligand 15 exhibited seven total contacts, including three backbone and seven sidechain interactions, with four polar interactions, one charged interaction and one donor interaction, interacting with residues A403, A292, A333, A293 and A288. Bar graphs accompanying the heat map provided additional information. The bar graph above the heat map showed the total interaction counts for each residue, identifying residues such as A400, A405 and A410 as critical interaction sites. The bar graph to the right depicts total interactions for each ligand, highlighting ligands with the highest number of interactions across residues. Hotspots, such as residues A398 to A410, showed significant interactions with multiple ligands, with ligand 15 displaying a strong interaction (red cell) with residue A376 (Table 3) (Fig. 5).

DFT analysis parameters for aripiprazole and selected ligands

Density Functional Theory (DFT) analysis was conducted to assess the electronic properties of the reference drug aripiprazole and two ligands, ligand 4 and ligand 12, using the RB3LYP method. The dipole moment, a measure of

molecular polarity, was highest for ligand 4 at 14.3364 Debye, indicating it is more polar than both aripiprazole (5.7280 Debye) and ligand 12 (7.4489 Debye). The HOMO (Highest Occupied Molecular Orbital) energy levels, expressed in atomic units (a.u.), showed ligand 12 with the lowest value at -0.24550 a.u., highlighting its superior stability in donating electrons compared to ligand 4 (-0.19845 a.u.) and aripiprazole (-0.21423 a.u.). Conversely, aripiprazole had the lowest LUMO (Lowest Unoccupied Molecular Orbital) energy at -0.01829 a.u., indicating it has the highest electron-accepting ability compared to ligand 4 (-0.04050 a.u.) and ligand 12 (-0.21412 a.u.). The energy gap (ΔE_{Gap}), representing the difference between HOMO and LUMO energy levels, identified ligand 12 as the most reactive compound with the smallest gap of 0.03138 a.u., followed by ligand 4 (0.04080 a.u.) and aripiprazole (0.19594 a.u.). In terms of total energy, which reflects molecular stability, aripiprazole emerged as the most stable, with the lowest value of -2116.63621998 a.u., compared to ligand 4 (-945.10298323 a.u.) and ligand 12 (-1127.56478021 a.u.). These results indicate that ligand 4 has the highest polarity, ligand 12 is the most reactive due to its small energy gap and aripiprazole is the most stable compound overall. These findings provide a comprehensive understanding of the electronic characteristics, stability and reactivity of the analyzed compounds (Table 4 and Fig. 6).

DISCUSSION

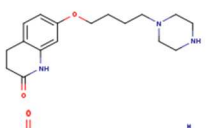
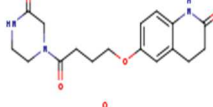
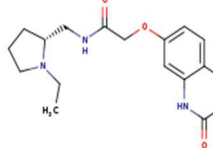
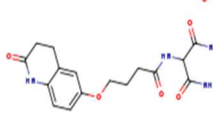
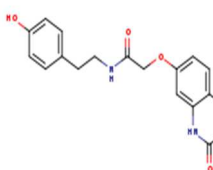
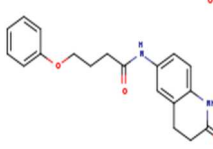
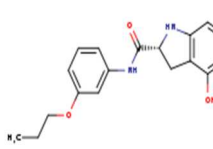
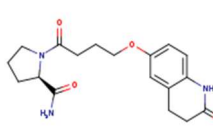
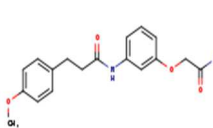
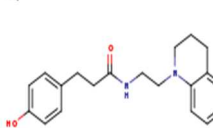
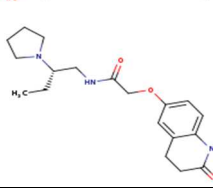
Of the many genetic variations of drug addiction discovered, the CHRNA5 cluster variants on chromosome 15 have received a lot of attention recently. It is noteworthy that mutations in this gene cluster have been connected to addiction. The polymorphism SNP rs16969968 seems to be the most interesting element in relation to drug addiction among all the significant variants in this cluster. When this polymorphism occurs, the amino acid at position 398 of the protein sequence changes from aspartate to asparagine (Bierut *et al.*, 2008). At position 398, asparagine (N) was substituted for aspartic acid (D) in order to compare the D398N mutation of the CHRNA5 protein to the wild-type structure.

While SIFT and PolyPhen-2 (with a score of 0.0004) predicted the D398N change in CHRNA5 as benign, the AlphaMissense heatmap flagged it as possibly pathogenic (score > 0.7), strengthening the case for using multiple predictive tools in assessing the risk. Structural models from AlphaFold, which were aligned with BLAST, showed that the mutation does cause a local change in the helical region of the receptor, confirming the models. The overall fold is preserved, but the substitution of aspartate, which is negatively charged, with a neutral asparagine at position 398 is likely to improve the intra-domain electrostatic and hydrogen-bonding interactions within the ligand-binding domain and thus further functional studies delineating receptor activity and ligand interaction would be valuable.

Table 1: Pharmacokinetic parameters of the selected ligands by SwissADME.

PROPERTIES	Water solubility		GI absorption		skin permeation		P-gp substrate		Bioviability		BBB permeability		CYP1A2 inhibitor		CYP2C19 inhibitor		CYP2C9 inhibitor		CYP2D6 inhibitor		CYP3A4 inhibitor	
	Absorption	solubility	Absorption	High	Absorption	permeation	Absorption	Yes	Absorption	0.55	Distribution	permeability	Metabolism	inhibitor	Metabolism	inhibitor	Metabolism	inhibitor	Metabolism	inhibitor	Metabolism	
Model Name																						
LIGAND 1	-2.24	Soluble	High	High	-7.35	Yes	Yes	0.55	No	No	No	No	No	No	No	No	No	No	Yes	No	No	
LIGAND 2	-1.65	Very soluble	High	High	-8.36	Yes	Yes	0.55	No	No	No	No	No	No	No	No	No	No	No	No	No	
LIGAND 3	-2.46	Soluble	High	High	-7.37	Yes	Yes	0.55	No	No	No	No	No	No	No	No	No	No	No	No	No	
LIGAND 4	-0.78	Very soluble	Low	Low	-9.33	No	No	0.55	No	0.55	No	No	No	No	No	No	No	No	No	No	No	
LIGAND5	-3.09	Soluble	High	High	-6.97	Yes	Yes	0.55	No	No	No	No	No	No	No	No	No	Yes	Yes	No	No	
LIGAND 6	-3.15	Soluble	High	High	-6.72	Yes	Yes	0.55	Yes	Yes	Yes	Yes	Yes	Yes	No	Yes	Yes	Yes	Yes	Yes	Yes	
LIGAND 7	-3.9	Soluble	High	High	-5.8	Yes	Yes	0.55	Yes	Yes	Yes	Yes	Yes	Yes	No	Yes	Yes	Yes	Yes	Yes	Yes	
LIGAND 8	-1.88	Very soluble	High	High	-8.2	Yes	Yes	0.55	No	0.55	No	No	No	No	No	No	No	No	No	No	No	
LIGAND 9	-2.84	Soluble	High	High	-6.97	No	No	0.55	No	0.55	No	No	No	No	No	No	No	Yes	Yes	No	No	
LIGAND 10	-3.83	Soluble	High	High	-5.94	Yes	Yes	0.55	Yes	Yes	Yes	Yes	Yes	Yes	No	Yes	No	Yes	Yes	No	No	
LIGAND 11	-2.81	Soluble	High	High	-7.08	Yes	Yes	0.55	Yes	0.55	No	No	No	No	No	No	No	Yes	Yes	No	No	
LIGAND 12	-2.46	Soluble	High	High	-7.37	Yes	Yes	0.55	Yes	0.55	No	No	No	No	No	No	No	Yes	Yes	No	No	
LIGAND 13	-3.9	Soluble	High	High	-5.74	No	No	0.55	No	0.55	Yes	Yes	Yes	Yes	No	No	No	Yes	Yes	Yes	Yes	
LIGAND 14	-1.88	Very soluble	High	High	-8.2	Yes	Yes	0.55	Yes	0.55	No	No	No	No	No	No	No	No	No	No	No	
LIGAND 15	-4.1	Moderately soluble	High	High	-5.74	No	No	0.55	No	0.55	Yes	Yes	Yes	No	No	No	No	Yes	Yes	Yes	Yes	
LIGAND 16	-1.85	Very soluble	High	High	-8.25	Yes	Yes	0.55	Yes	0.55	No	No	No	No	No	No	No	No	No	No	No	
LIGAND 17	-3.47	Soluble	High	High	-6.52	Yes	Yes	0.55	Yes	0.55	Yes	Yes	Yes	Yes	Yes	Yes	Yes	Yes	Yes	No	No	
LIGAND 18	-2.65	Soluble	High	High	-7.04	Yes	Yes	0.55	Yes	0.55	Yes	Yes	No	No	No	No	No	Yes	Yes	No	No	
LIGAND 19	-2.15	Soluble	High	High	-7.68	Yes	Yes	0.55	Yes	0.55	No	No	No	No	No	No	No	No	No	No	No	
LIGAND 20	-3.11	Soluble	High	High	-6.54	No	No	0.55	No	0.55	No	No	No	No	No	No	No	Yes	Yes	Yes	Yes	

Table 2: Ligands 2D structures, SMILES and their docking scores

Ligands	2D Structure	Canonical SMILES	Docking Score	Glide Score
LIGAND 1		<chem>O=C1CCc2c(N1)cc(cc2)OCCCCN1CCNCC1</chem>		
LIGAND 2		<chem>O=C1NCCN(C1)C(=O)CCCOc1ccc2c(c1)CCC(=O)N2</chem>	-2.685	-2.685
LIGAND 3		<chem>CCN1CCC[C@@H]1CNC(=O)COc1ccc2c(c1)NC(=O)CC2</chem>	-1.944	-1.946
LIGAND 4		<chem>O=C(NC(C(=O)N)C(=O)N)CCCOc1ccc2c(c1)CCC(=O)N2</chem>	-2.774	-2.909
LIGAND 5		<chem>O=C(COc1ccc2c(c1)NC(=O)CC2)NCCc1ccc(cc1)O</chem>	-0.478	-0.478
LIGAND 6		<chem>O=C(Nc1ccc2c(c1)CCC(=O)N2)CCCOc1ccccc1</chem>	0.375	0.375
LIGAND 7		<chem>CCCOc1cccc(c1)NC(=O)[C@@H]1Nc2c(C1)c(O)ccc2</chem>	-2.198	-2.198
LIGAND 8		<chem>O=C1CCc2c(N1)ccc(c2)OCC(=O)N1CCC[C@@H]1C(=O)N</chem>	-2.001	-2.001
LIGAND 9		<chem>COc1ccc(cc1)CCC(=O)Nc1cccc(c1)OCC(=O)N</chem>	-2.125	-2.125
LIGAND 10		<chem>O=C(CCc1ccc(cc1)O)NCCN1CCCCc2c1ccccc2</chem>	-0.336	-0.336
LIGAND 11		<chem>CC[C@H](N1CCCC1)CNC(=O)COc1ccc2c(c1)CCC(=O)N2</chem>	-1.618	-1.621

Continue...Table 2

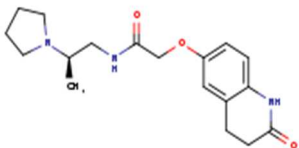
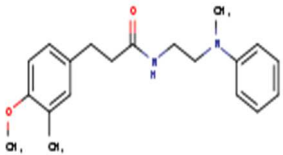
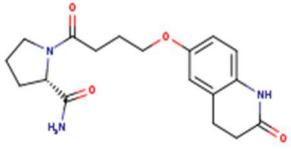
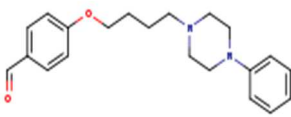
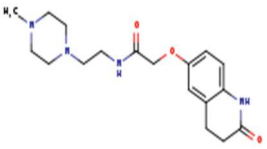
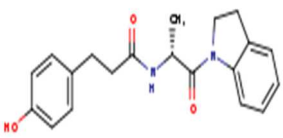
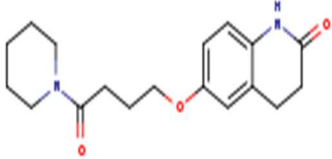
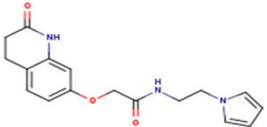
LIGAND 12		<chem>O=C(COc1ccc2c(c1)CCC(=O)N2)NC[C@H](N1CCCC1)C</chem>	-3.034	-3.039
LIGAND 13		<chem>COc1ccc(cc1C)CCC(=O)NCCN(c1ccccc1)C</chem>	-1.598	-1.599
LIGAND 14		<chem>O=C1CCc2c(N1)ccc(c2)OCCCC(=O)N1CCC[C@H]1C(=O)N</chem>	-2.129	-2.129
LIGAND 15		<chem>O=Cc1ccc(cc1)OCCCCN1CCN(CC1)c1ccccc1</chem>	-0.769	-0.905
LIGAND 16		<chem>CN1CCN(CC1)CCNC(=O)Coc1ccc2c(c1)CCC(=O)N2</chem>	-1.761	-1.808
LIGAND 17		<chem>O=C(N[C@@H](C(=O)N1CCc2c1ccccc2)C)CCc1ccc(cc1)O</chem>	0.123	0.122
LIGAND 18		<chem>O=C1CCc2c(N1)ccc(c2)OCCCC(=O)N1CCCCC1</chem>	-1.883	-1.883
LIGAND 19		<chem>O=C(COc1ccc2c(c1)NC(=O)CC2)NCCn1ccccc1</chem>	-1.896	-1.896

Table 3: Interaction heat map analysis of ligand-residue fingerprinting in Maestro.

LIGAND	Total contact	Total backbone	Total polar	Total charged	Total sidechain	Total donor	Interaction names
LIGAND 12	6	5	5	2	6	2	A:400, A:287, A:329, A:300, A:287
LIGAND 4	5	2	4	2	5	2	A:300, A:310, A:327, A:315, A:314
LIGAND 2	6	2	5	3	6	2	A:401, A:330, A:289, A:331, A:288
LIGAND1	5	4	4	2	5	1	A:402, A:290, A:332, A:291, A:287
LIGAND 15	7	3	4	1	7	1	A:403, A:292, A:333, A:293, A:288

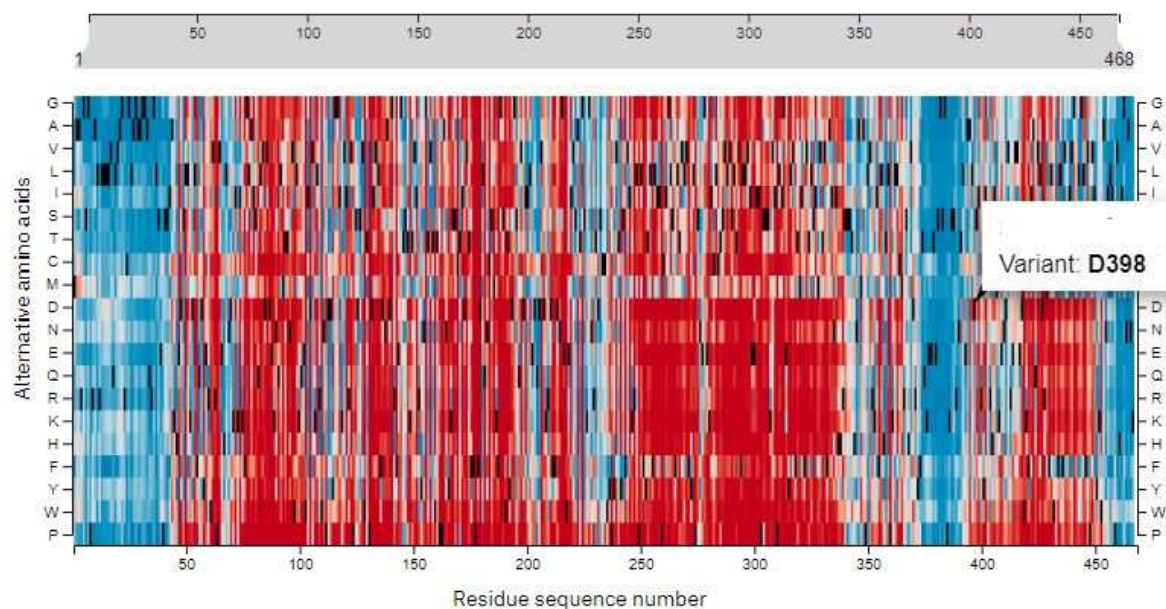


Fig. 1: The AlphaMissense pathogenicity heatmap predicts the mutation as pathogenic.

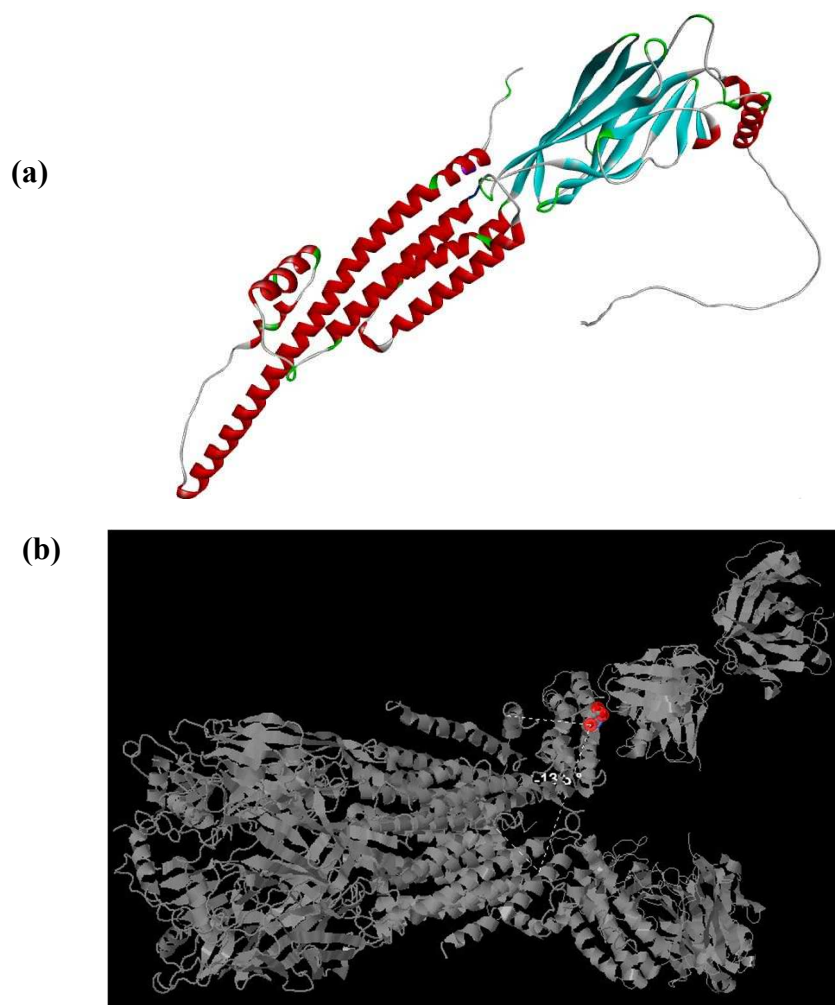


Fig. 2: (a) Wild-type structure of the CHRNA5 protein. (b) Predicted structure of the mutated CHRNA5 protein (D398N). The red spot indicates the mutation site.

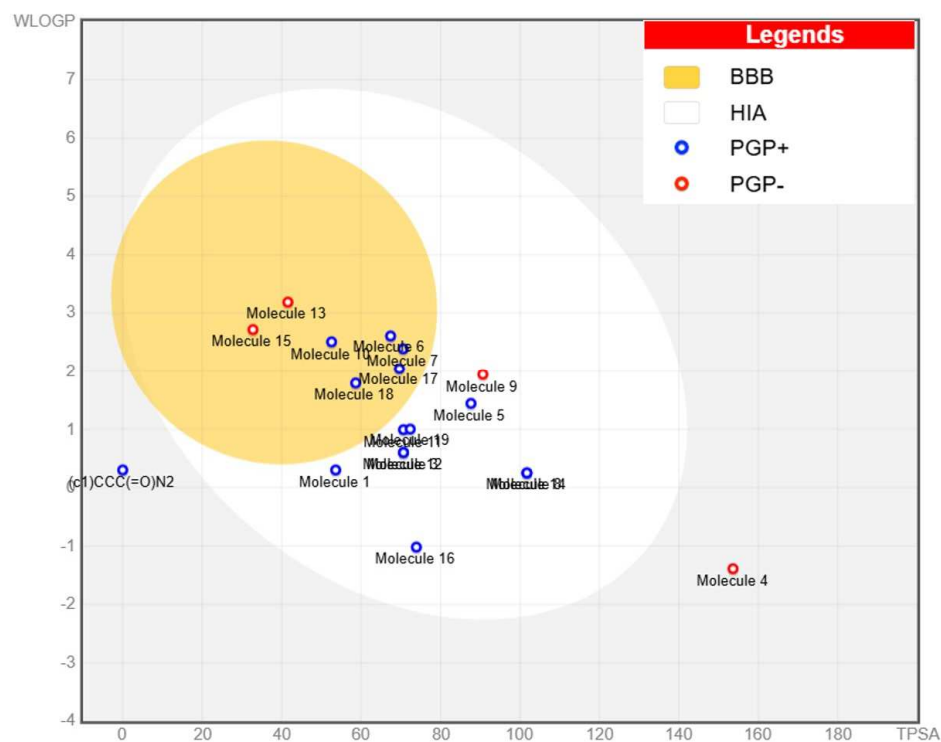


Fig. 3: The "BOILED-Egg" plot from SwissADME predicts gastrointestinal absorption (HIA) and blood-brain barrier (BBB) permeability.

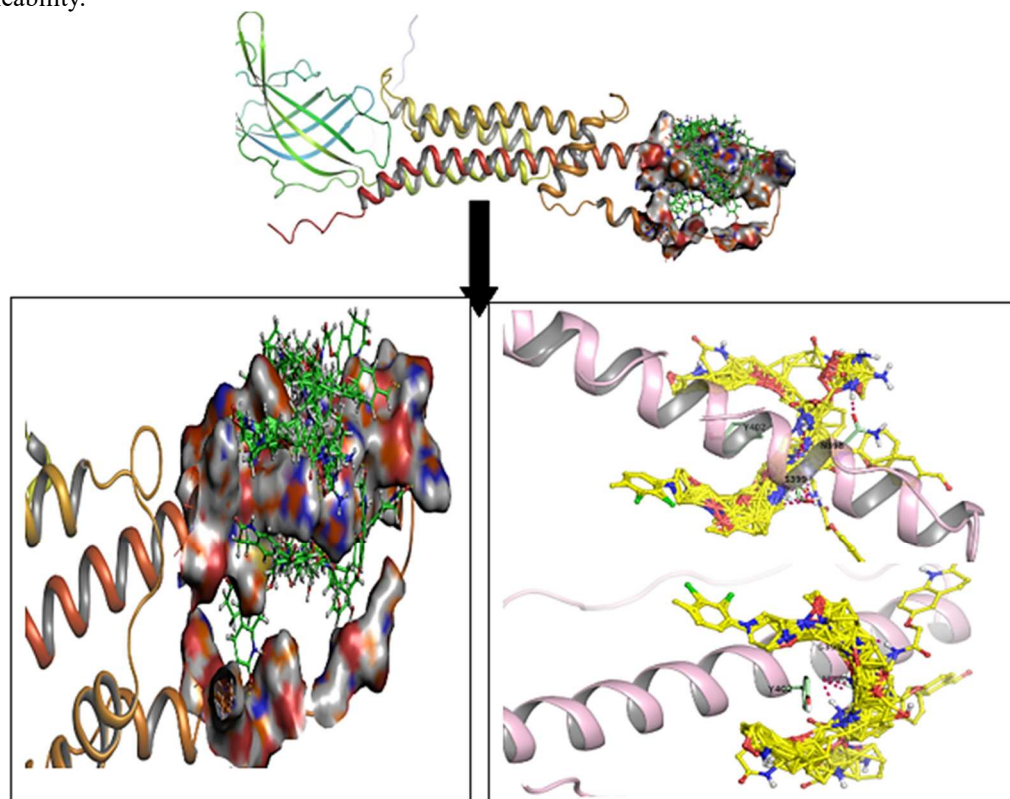


Fig. 4: 3D structural visualization of CHRNAS5 docked with aripiprazole by PyMOL

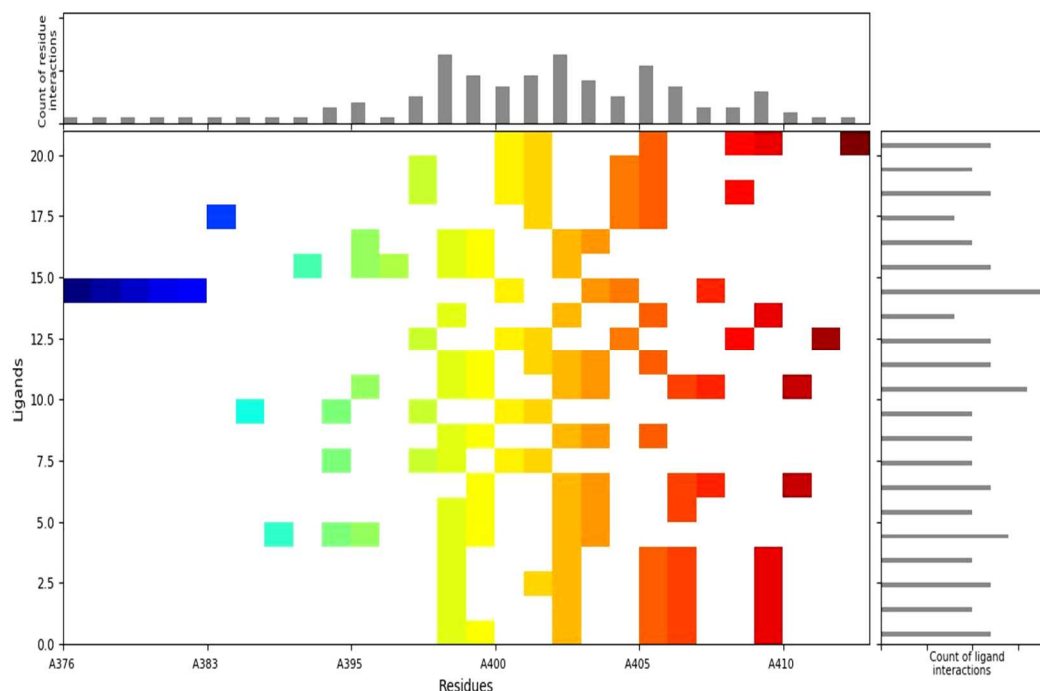


Fig. 5: Interaction heat map analysis of ligand-residue fingerprinting in Maestro.

Table 4: DFT analysis parameters of the Ligands and reference drug.

Parameters	Aripiprazole	Ligand 4	Ligand 12
Dipole moment (Debye)	5.7280 Debye	14.3364 Debye	7.4489 Debye
HOMO (a.u.)	-0.19038	-0.20709	-0.24550
LUMO (a.u.)	-0.01829	-0.01432	0.21412
Energy Gap (ΔE_{Gap})	0.17209	0.19277	0.03138
Total Energy	-2116.63621998 a.u.	-1210.07749855 a.u.	-1068.89792610 a.u.
Calculation Method	RB3LYP	RB3LYP	RB3LYP

Functional studies have demonstrated that D398N variant leads to reduced receptor function, impacting nicotine response and increased addiction risk (Tammimäki *et al.*, 2012). Comprehending these structural alterations is essential for examining the protein's function in addiction and the consequences for therapeutic approaches. Integrating computational predictions with experimental validations remains crucial for accurate assessment of variant pathogenicity (Ryan-Phillips *et al.*, 2024).

To find viable treatment possibilities, twenty substances were first carefully examined. From the ADMET analysis presented in table 1 and the BOILED-Egg plot (Fig. 3), it was noticed that most of the ligands had favorable pharmacokinetic properties. In most cases, compounds had high permeability and gastrointestinal solubility, which aligns with Lipinski's Rule of 5, as well as the absence of PAINS alerts. The BOILED-Egg plot effectively categorized compounds based on their gastrointestinal absorption and BBB permeability, demonstrating its utility

in drug discovery processes (Afzal *et al.*, 2024). The BOILED-Egg plot validated that 19 ligands were placed within the white zone, signifying high intestinal permeability and only a couple entered the yellow zone, implicating poor BBB permeability, desirable attribute for non-CNS drug hopefuls. Ligands 2, 8, 11, 12 and 14 were outstanding because they exhibited high solubility, good GI absorption, non-CYP enzyme inhibition and lack of structural toxicity warnings, thus showing great potential for development.

Recent studies have reinforced the significance of CHRNA5 D398N mutation in substance dependence and its potential as therapeutic agent (Brynildsen and Blendy, 2021). The functional analyses have demonstrated that this mutation alters the function of $\alpha 5$ -containing nAChRs, impacting neural circuits involved in reward, aversion and attention (Brynildsen and Blendy, 2021). The top 20 compounds were selected as ligands after the ADMET analysis and they were compared to the reference drug,

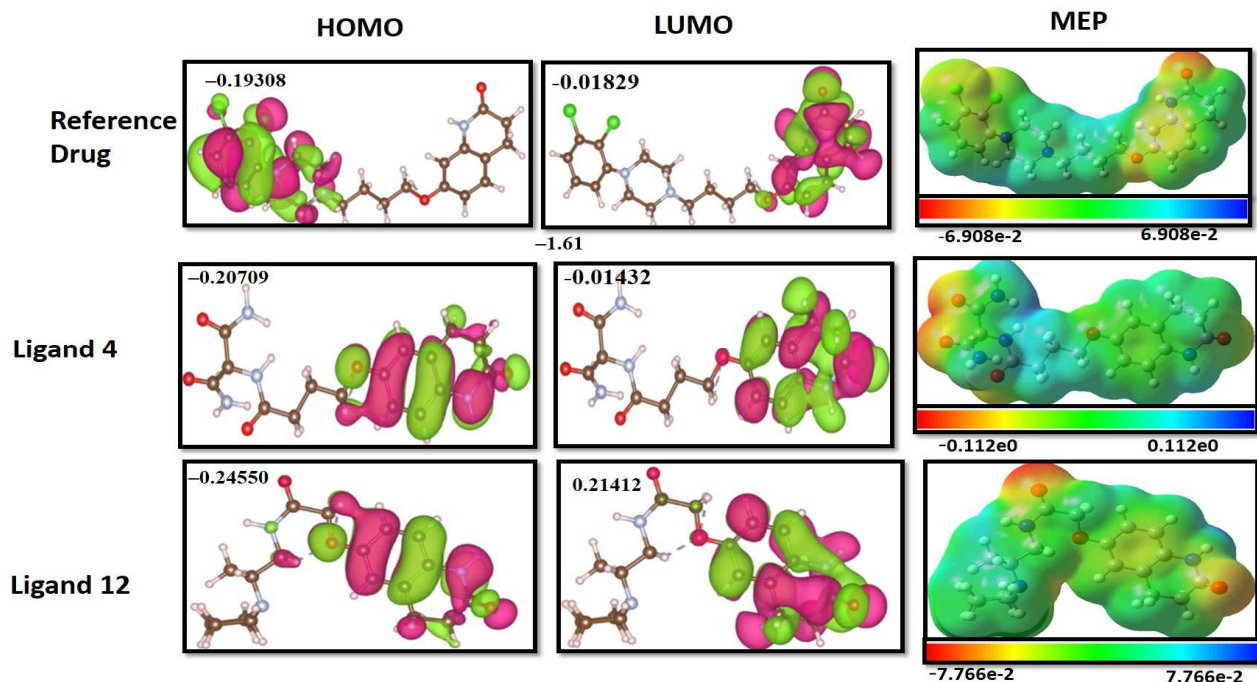


Fig. 6: DFT analysis parameters for aripiprazole and selected ligands

aripiprazole. The molecular docking study showed that a number of candidate ligands indicated higher binding affinities towards the mutated CHRNA5 protein than reference drug aripiprazole, which had a score of -1.993. Most notably, ligand 12 indicated the highest value of docking score -3.034, followed by ligands 4 (-2.774), 2 (-2.685) and 1 (-2.450), which reflected increased potential for interaction with the modified binding site. The D398N mutation in a transmembrane or ligand-binding region likely impacted the electrostatic atmosphere due to replacement of a negative charge aspartic acid by an uncharged asparagine and thus altered the orientation of ligand as well as its affinity. Interaction heat map and fingerprint analysis also validated these findings, indicating that best ligands like 12, 4, 2, 1 and 15 interacted with key residues (e.g., A400, A287, A300) through polar, charged and donor interactions. Ligand 15 had the highest number of overall contacts, supporting its potential to be an important binder.

These in silico verifications, such as RMSD values less than 2 Å for redocking, highlight the structural compatibility and interaction specificity of these ligands, making them good candidates for experimental validation against mutated CHRNA5-linked conditions like nicotine dependence or neuropsychiatric disorders. The polymorphism SNP rs16969968 seems to be the most interesting element in relation to drug addiction out of all the notable variants in this cluster. New efforts to explore the molecular pathways via which genetic variations in this region influence drug addiction and related symptoms have been prompted by genetic studies.

A study was performed in which three polymorphic variants were examined, rs16969968 in the CHRNA5 gene, rs578776 in the CHRNA3 gene and rs1051730 in the CHRNA3 gene in individuals with nicotine addiction. The frequency of genotypes for the CHRNA3 gene's rs1051730 polymorphism showed a statistically significant difference ($\chi^2 = 6.704$, $p = 0.035$). The group of subjects who were dependent on nicotine had a statistically significantly higher frequency of the T/T genotype. Among the identified haplotypes, rs16969968, rs578776 and rs1051730, the G-T-T and G-C-T haplotypes were exclusive to the study group. Statistical significance was observed for the G-T-T haplotype and the G-C-T haplotype with respect to frequency differences. According to the study, the novel haplotypes G-T-T and G-C-T were associated with addiction despite having incredibly rare mutations in CHRNA3 (Chmielowiec *et al.*, 2022). A 2015-2019 study examined the response of smokers with varying CHRNA5 genotypes to smoking cessation therapies. The results indicated that African American smokers with the GG genotype reacted favorably to combination nicotine replacement therapy, whereas those with GA/AA genotypes benefited from varenicline. This indicates that treatment plans tailored to CHRNA5 genotype may improve smoking cessation rates (Chen LS *et al.*, 2020). Strong evidence suggests that heredity has a major role in drug abuse. Cocaine, alcohol, nicotine and opioid addiction have all been connected in human cultures to the single nucleotide polymorphism (SNP) D398N in the CHRNA5 gene. One study presented an overview of studies conducted on cell lines, animal models and humans.

According to the data collected, the Chrna5 SNP has a general, non-substance-specific impact on how people react to dangerous drugs. This discovery has significant ramifications for our comprehension of the cholinergic system's function in reward and the susceptibility of addiction (Brynildsen and Blendy, 2021). Additionally, our research showed that D398N functions as a hotspot mutation in the CHRNA5 gene in drug addicts. Another study in which fifteen SNPs were found in the CHRNA5, CHRNA3 and CHRNB4 genes was conducted in Jordan (Al-Eitan *et al.*, 2024). The study relates with our study where rs16969968 mutation was found to play a key role in individuals affected with drug overuse.

Recent studies have demonstrated the utility of DFT in drug design, particularly in assessing electronic properties that influence molecular behavior (Ayub *et al.*, 2025). The DFT analysis found different electronic profiles of reference drug, aripiprazole, ligand 4 and ligand 12. ligand 4 had the greatest dipole moment with high polarity and ligand 12 had the least energy gap with high chemical reactivity. Aripiprazole had the least total energy with better thermodynamic stability. All these indicate that ligand 4 can improve solubility, ligand 12 can be more reactive in biological media and aripiprazole is the most stable compound in general.

The current investigation also revealed the use of aripiprazole and several other ligands as antipsychotic medications for the recovery of abusers. Aripiprazole is gradually replacing first-generation antipsychotics due to its superior side effect profile (Hirsch and Pringsheim, 2016). The U.S. Food and Drug Administration has approved aripiprazole, a third-generation atypical antipsychotic, for the treatment of bipolar disorder, schizophrenia and significant depression that is resistant to treatment. Its primary mode of action seems linked to partial agonism at the dopamine D2 receptor. Aripiprazole may, however, act through agonism, partial agonism, or antagonism at both dopamine and serotonin receptors, according to relatively recent pre-clinical studies. Our study also highlights the role of aripiprazole as an antipsychotic drug. Aripiprazole clinical trials in alcoholics have yielded mixed but encouraging outcomes.

Aripiprazole may be helpful for neuropsychiatric disorders where the main cause is a dysregulation of reward and impulsivity, such as alcoholism, because of its potential impact on frontal-subcortical circuits that support reward/craving and impulsive behavior. A study was conducted suggesting that more randomized controlled trials be created at suitable dosages to better understand aripiprazole's potential significance as a treatment option. It also argues that aripiprazole may have a role in the treatment of alcoholism (Vergne and Anton, 2010). Based on docking scores and ADMET analysis, our study showed that several other medications had better effects than aripiprazole when used as therapeutic agents. Further

investigation into the CHRNA5 gene in abusers and early rehabilitation treatment is still necessary. The genetic analysis of the CHRNA5 gene and the mutational role of D398N are highlighted in this study's conclusion, emphasizing the importance of accurate variant identification for prognosis and genetic consultations. The identification of many mutations and the investigation of different therapeutic techniques highlight the potential for customised treatment approaches. Even with great advancements, more research is still required to create efficient therapies and enhance the lives of drug addicts.

CONCLUSION

The pivotal role of the CHRNA5, specifically the D398N mutation (rs16969968), in drug addiction is highlighted by this study as a genetic marker for susceptibility and a possible therapeutic target. Several ligands with higher binding affinities to the mutant CHRNA5 protein than the reference drug, aripiprazole, were found by means of a comprehensive computational method that comprised Density Functional Theory (DFT) calculations, molecular docking and ADMET analysis. By demonstrating superior binding affinities, polarity and reactivity through docking scores, interaction studies and energy gap measurements, ligands like ligand 12 and ligand 4 showed promise as new therapeutic possibilities. Although aripiprazole's stability and efficacy in treating addiction-related neuropsychiatric symptoms make it a viable therapeutic option, the discovery of ligands with improved features highlights the significance of investigating alternative therapies.

In addition to highlighting the significance of genetic screening for CHRNA5 variations in determining addiction susceptibility, this work opens the door for early rehabilitation interventions and individualized treatment plans. However, the lack of *in-vitro* and *in-vivo* validation limits the translational relevance of these findings. Future research should aim to validate these findings experimentally and elucidate the molecular mechanisms by which CHRNA5 mutations influence drug addiction, ultimately guiding development of targeted therapies, aiming to improve clinical outcomes for individuals affected by drug addiction.

Acknowledgement

The authors extend their appreciation to Northern Border University, Saudi Arabia, for supporting this work.

Authors' contributions

Conceptualization and study design: Mohd Imran, Imran Waheed, and Muhammad Umer Khan

Data curation and analysis: Maria Kafayat, Lina Eltaib, and Saooda Ibrahim

Molecular docking and in silico modeling: Abdullah R. Alzahrani and Mohd Imran

Genetic interpretation and bioinformatics validation: Muhammad Umer Khan and Saooda Ibrahim

Manuscript drafting: Mohd Imran and Maria Kafayat
 Critical revision and scientific supervision: Imran Waheed, Howayada Mahany Mostafa, and Muhammad Umer Khan
 Final approval of the manuscript: All authors read and approved the final version of the manuscript.

Funding

The work is funded by the Northern Border University, Saudi Arabia, through project number (NBU-CRP-2025-2043).

Data availability statement

All data generated or analyzed during this study are included in the main manuscript file and its supplementary information files. Structural and sequence data used in this study were retrieved from publicly accessible databases, including UniProt, NCBI Gene, and the AlphaFold Protein Structure Database.

Ethical approval

The study obtained a bioethical clearance approval and certificate from the Bioethics Committee of the University of Lahore (ethical approval No. IMBB/24/BBBC/494-B). All procedures conducted in the current research with human participants adhered to the ethical standards set by the institutional and/or national research committee, as well as the principles highlighted in the 1964 Declaration of Helsinki, along with its consequent amendments and comparable ethical outlines.

Conflicts of interest

The authors have no conflict of interest in this publication.

Supplementary data

<https://www.pjps.pk/uploads/2025/12/SUP1764845960.pdf>

REFERENCES

- Al-Eitan L, Shatnawi M and Alghamdi M (2024). Investigating CHRNA5, CHRNA3 and CHRNA4 variants in the genetic landscape of substance use disorder in Jordan. *BMC Psychiatry*, **24**(1): 436.
- Aroche AP, Rovaris DL, Grevet EH, Stolf AR, Sanvicente-Vieira B, Kessler FHP and Schuch JB (2020). Association of CHRNA5 gene variants with crack cocaine addiction. *Neuromol. Med.*, **22**(3): 384-390.
- Afzal AH, Alam O, Zafar S, Alam MA, Ahmed K, Khan J, Khan R, Shahat AA and Alhalmi A (2024). Application of machine learning for the prediction of absorption, distribution, metabolism and excretion (ADME) properties from *Cichorium intybus* plant phytochemicals. *Processes*, **12**(11): 2488.
- Ayub MA, Tyagi AR, Srivastava SK and Singh P (2025). Quantum DFT analysis and molecular docking investigation of various potential breast cancer drugs. *J. Mater. Chem. B.*, **13**(1): 218-238.
- Bierut LJ, Stitzel JA, Wang JC, Hinrichs AL, Grucza RA, Xuei X and Goate AM (2008). Variants in nicotinic receptors and risk for nicotine dependence. *Am. J. Psychiatry*, **165**(9): 1163-1171.
- Brynildsen JK and Blendy JA (2021). Linking the CHRNA5 SNP to drug abuse liability: From circuitry to cellular mechanisms. *Neuropharmacol.*, **186**: 108480.
- Bao F, Li Y, Liu W, She C, Chen K, Li L and Jin S (2020). Density Functional Theory (DFT) study on the structures and energetic properties of isomers of tetranitro-bis-1,2,4-triazoles. *ACS Omega*, **5**: 19464–19468.
- Chaity NI and Apu MNH (2022). CHRNA5 rs16969968 and CHRNA3 rs578776 polymorphisms are associated with multiple nicotine dependence phenotypes in Bangladeshi smokers. *Heliyon*, **8**(7): e09947.
- Chaity NI, Sultana TN, Hasan MM, Shrabonee II, Nahid NA, Islam MS and Apu MNH (2021). Nicotinic acetylcholine gene cluster CHRNA5-A3-B4 variants influence smoking status in a Bangladeshi population. *Pharmacol. Rep.*, **73**(2): 574-582.
- Chmielowiec K, Chmielowiec J, Strońska-Pluta A, Trybek G, Śmiarowska M, Suchanecka A, Grzywacz A (2022). Association of Polymorphism CHRNA5 and CHRNA3 Gene in People Addicted to Nicotine. *Int. J. Environ. Res. Public Health*, **19**(17): 10478.
- Chen LS, Baker TB, Miller JP, Bray M, Smock N, Chen J, Stoneking F, Culverhouse RC, Saccone NL, Amos CI, Carney RM, Jorenby DE and Bierut LJ (2020). Genetic variant in CHRNA5 and response to varenicline and combination nicotine replacement in a randomized placebo-controlled trial. *Clin. Pharmacol. Ther.*, **108**(6): 1315-1325.
- Flanagan SE, Patch AM and Ellard S (2010). Using SIFT and PolyPhen to predict loss-of-function and gain-of-function mutations. *Genet. Test. Mol. Biomarkers*, **14**(4): 533-537.
- Hirsch LE and Pringsheim T (2016). Aripiprazole for autism spectrum disorders (ASD). *Cochrane. Database Syst. Rev.*, **1**(6): Cd009043.
- Icick R, Forget B, Cloez-Tayarani I, Pons S, Maskos U and Besson M (2020). Genetic susceptibility to nicotine addiction: Advances and shortcomings in our understanding of the CHRNA5/A3/B4 gene cluster contribution. *Neuropharmacol.*, **177**: 108234.
- Islam S, Hussain EA, Shujaat S, Khan MU, Ali Q, Malook SU and Ali D (2024). Antibacterial potential of Propolis: Molecular docking, simulation and toxicity analysis. *AMB Express*, **14**(1): 81.
- Maestro S (2020). Maestro. *Schrodinger, LLC, New York, NY, 2020*, p.682.
- Milne GW (2010). Software review of ChemBioDraw 12.0: ACS Publications.
- Muderrisoglu A, Babaoglu E, Korkmaz ET, Kalkisim S, Karabulut E, Emri S and Babaoglu MO (2022). Comparative assessment of outcomes in drug treatment for smoking cessation and role of genetic

- polymorphisms of human nicotinic acetylcholine receptor subunits. *Front Genet.*, **13**: 812715.
- Moran L, Phillips K, Kowalczyk W, Ghitz U, Agage D, Epstein D and Preston K (2017). Aripiprazole for cocaine abstinence: a randomized-controlled trial with ecological momentary assessment. *Behav. Pharmacol.*, **28**(1): 63–73.
- Rauf A, Naz S, Khan MU, Zahid T, Ahmad Z, Akram Z and Alamri AS (2025). Aldose reductase inhibitory evaluation and in silico studies of bioactive secondary metabolites isolated from *Fernandoa. adenophylla* (Wall. ex G. Don). *J. Mol. Struct.*, **1328**(1): 141308.
- Ryan-Phillips F, Henahan L, Ramdas S, Palace J, Beeson D and Dong YY (2024). Assessing the utility of colabfold and alphamissense in determining missense variant pathogenicity for congenital myasthenic syndromes. *Biomedicines*, **12**(11): 2549.
- Sansone L, Milani F, Fabrizi R, Belli M, Cristina M, Zagà V and Russo P (2023). Nicotine: From Discovery to biological effects. *Int. J. Mol. Sci.*, **24**(19): 14570.
- Schlaepfer IR, Hoft NR, Collins AC, Corley RP, Hewitt JK, Hopfer CJ and Ehringer MA (2008). The CHRNA5/A3/B4 gene cluster variability as an important determinant of early alcohol and tobacco initiation in young adults. *Biol. Psychiatry.*, **63**(11): 1039-1046.
- Scholze P and Huck S (2020). The $\alpha 5$ Nicotinic acetylcholine receptor subunit differentially modulates $\alpha 4\beta 2(*)$ and $\alpha 3\beta 4(*)$ receptors. *Front Synaptic Neurosci.*, **12**: 607959.
- Shan MA, Khan MU, Ishtiaq W, Rehman R Khan, S Javed, MA and Ali Q (2024). In silico analysis of the Val66Met mutation in BDNF protein: implications for psychological stress. *AMB Express*, **14**(1): 11.
- Silvarajoo S, Osman UM, Kamarudin KH, Razali MH, Yusoff HM, Bhat IUH and Juahir Y (2020). Dataset of theoretical Molecular Electrostatic Potential (MEP), Highest Occupied Molecular Orbital-Lowest Unoccupied Molecular Orbital (HOMO-LUMO) band gap and experimental cole-cole plot of 4-(ortho-, meta- and para-fluorophenyl) thiosemicarbazide isomers. *Data Brief.*, **32**: 106299.
- Sim NL, Kumar P, Hu J, Henikoff S, Schneider G and Ng PC (2012). SIFT web server: Predicting effects of amino acid substitutions on proteins. *Nucleic acids research*, **40**(W1): W452-W457.
- Systèmes D (2021). Discovery studio visualizer. **16**(1): 15350.
- Tammimaki A, Herder P, Li P, Esch C, Laughlin JR, Akk G and Stitzel JA (2012). Impact of human D398N single nucleotide polymorphism on intracellular calcium response mediated by $\alpha 3\beta 4\alpha 5$ nicotinic acetylcholine receptors. *Neuropharmacol.*, **63**(6): 1002-1011.
- Uniyal A and Mahapatra MK (2022). Targeting SARS-CoV-2 main protease: Structure based virtual screening, in silico ADMET studies and molecular dynamics simulation for identification of potential inhibitors. *J. Biomol. Struct. Dyn.*, **40**(8): 3609-3625.
- Vergne D E and Anton RF (2010). Aripiprazole: A drug with a novel mechanism of action and possible efficacy for alcohol dependence. *CNS Neurol. Disord. Drug Targets*, **9**(1): 50-54.
- Yang K, McLaughlin I, Shaw JK, Quijano-Cardé N, Dani JA and De Biasi M (2023). CHRNA5 gene variation affects the response of VTA dopaminergic neurons during chronic nicotine exposure and withdrawal. *Neuropharmacol.*, **235**: 109547.